Progress In Electromagnetics Research B, Vol. 13, 409–431, 2009

SIMULATING WIDE BAND RADAR RESPONSE FROM PEC TARGETS USING PHASE EXTRACTED BASIS FUNCTIONS

S. Yan, S. He, Z. Nie, and J. Hu

Department of Microwave Engineering
University of Electronic Science and Technology of China
No. 4, Sec. 2, N. Jianshe Rd., Chengdu, Sichuan 610054, P. R. China

Abstract—In this paper, we first review the Phase Extracted (PE) basis functions by recalling the derivation which shows that the induced current on a PEC surface has the propagating phase factor the same as the incident wave in a scattering problem. The wide band characteristic of this PE basis functions has been investigated by demonstrating that very wide band radar response from PEC objects can be simulated accurately by using PE bases, only based on a single coarse mesh grid. Besides, the resulted current coefficients are shown to vary slowly and smoothly with frequency changing and can be interpolated and extrapolated in very wide band easily. The piecewise cubic Hermite interpolation/extrapolation method with respect to the current coefficients is used to obtain the coefficients in the frequency band of interest. Numerical examples demonstrate very good accuracy and high efficiency in wide band radar response prediction in terms of the amplitude of the scattering field as well as its phase distribution.

1. INTRODUCTION

In the field of Computational Electromagnetics (CEM), wide band radar response from PEC targets attracts much attention from researchers. Generally speaking, both time domain and frequency domain methods can be used to calculate the wide band response. As methods that can calculate wide band response directly, the time domain methods, such as FDTD and TDIE, can rarely be used in the applications of the large targets in real world due to the high computational and storage complexities.

Corresponding author: S. Yan (syan@uestc.edu.cn).

On the other hand, frequency domain methods have to calculate the responses frequency by frequency, and then apply fast Fourier transform to obtain time domain result, which definitely lower the practicability of such kind of methods.

To overcome these problems, many wide band algorithms have been developed. These algorithms usually consist of two aspects of problem: the direct calculations at the frequency samples in a wide frequency range and the reconstructions at the other frequency points. In order to develop a wide band method that can deal with electrically large objects in real world, one has to make efforts in both aspects.

Several data reconstruction methods, such as the asymptotic waveform evaluation (AWE)/Padé approximation [1, 2], Cauchy method [3–5], model-based parameter estimation (MBPE) [6–8], impedance matrix interpolation [9, 10], and model order reduction [11] etc., have been developed to obtain the scattering results at the points beyond the frequency samples in the bandwidth without the direct calculation.

In the above methods, AWE/Padé approximation method [1, 2] needs to generate a full impedance matrix and calculate its inverse and nth order derivative, which is very time and memory consuming. Cauchy method [3–5] uses the ratio of two rational functions to approximate the highly oscillatory function directly, which may compromise the accuracy especially in electrically large problems. MBPE [6–8] and impedance matrix interpolation methods [9, 10] need to calculate the full impedance matrix. The latter needs much more memory to store several full impedance matrices in order to save computational time in the interpolation procedure.

Moreover, the above methods in formulation-domain modeling based on the fulfilled impedance matrix are not available in Multilevel Fast Multipole Algorithm (MLFMA) [12–15]. On the other hand the methods in solution-domain modeling suffer from the difficulty of accuracy due to the fast oscillating of the data.

A simple interpolation/extrapolation method for wide band prediction is presented in [16, 17]. The main idea of the method is to "normalize" the current coefficient obtained using either MoM [18–23] or MLFMA [12–15] by an exponential function which is assumed to be the frequency dependence factor of the induced current. After this normalization, the residual part of current varies slowly via frequency so that it can be interpolated and extrapolated with ease. However, in order to obtain the accurate result at each frequency, the obstacle has to be meshed at the highest frequency. Thus, the number of unknown cannot be reduced at each sample frequency, even at the lowest frequency. Obviously, this is not so cost-effective.

In [24], a Phase Extracted (PE) basis function has been proposed and a matrix sparsification and an impedance prediction technique have been introduced in MoM. The differences between PE basis functions and the existing methods have also been discussed in that paper. In this paper, a method for wide band scattering based on the Phase Extracted Basis Functions is introduced. From theoretical derivation, it can be shown that the induced current in a scattering problem has a phase dependence the same as the incident wave. Therefore, by introducing this phase dependence into basis function, it can lead to a residual amplitude part which is slowly varying. At least two benefits can be observed evidently by use of PE bases in wide band analysis. First, the current coefficients, which only represent the amplitude and the initial phase of the induced current, vary very slowly and smoothly with changing frequency. Secondly, owing to the wide band characteristic of the PE bases, the scattering from PEC targets, including the amplitude distribution of the far field (RCS) and the corresponded phase distribution, can be calculated with high accuracy only based on the single mesh grid produced at lowest frequency of interest.

This paper is organized as follows. The phase dependence of induced current in a PEC scattering problem is derived, and Phase Extracted basis functions are reviewed briefly in Section 2. In Section 3, the wide band characteristic of PE bases is examined. A simple interpolation/extrapolation method based on the current coefficients obtained from PE bases is introduced in Section 4. Some wide band calculation results are given in Section 5 to demonstrate the high efficiency and good accuracy of this method. After some discussions in Section 6, the conclusion is finally made in Section 7.

2. PHASE EXTRACTED BASIS FUNCTIONS

To get the phase dependence of the induced surface current on the PEC surface in scattering problems, we begin with the Maxwell's equation:

$$\nabla \times \mathbf{E} = i\omega\mu\mathbf{H}, \tag{1}$$

the surface equivalence theorem:

$$\mathbf{J} = \hat{\mathbf{n}} \times \mathbf{H}, \tag{2}$$

and the constitutive relation:

$$\mathbf{D} = \varepsilon\mathbf{E} \tag{3}$$

The induced current has the following relationship with electric flux from above expressions:

$$\mathbf{J} = \frac{1}{i\omega\mu\varepsilon}\hat{\mathbf{n}} \times \nabla \times \mathbf{D}, \tag{4}$$

where ε and μ are constant in homogeneous background media. Curl $\mathbf{D}$ can then be expressed in the local coordinate as:

$$\begin{aligned} \nabla \times \mathbf{D} &= \left(\nabla_t + \hat{\mathbf{n}}\frac{\partial}{\partial n}\right) \times (\mathbf{D}_t + \hat{\mathbf{n}}D_n) \\ &= \nabla_t \times \mathbf{D}_t + \nabla_t \times \hat{\mathbf{n}}D_n + \hat{\mathbf{n}} \times \frac{\partial \mathbf{D}_t}{\partial n} \end{aligned} \tag{5}$$

where $\hat{\mathbf{n}}$ stands for the normal direction of the PEC surface at any given point $\mathbf{r}$; D_n and $\mathbf{D}_t$ are normal component and tangential component of electric flux, respectively.

Note that $\nabla_t \times \mathbf{D}_t = 0$ because the partial derivative is taken on the object's surface where $\mathbf{D}_t \equiv 0$ due to the boundary condition at PEC surfaces. Hence,

$$\mathbf{J} = \frac{1}{i\omega\mu\varepsilon}\left(\nabla_t D_n - \frac{\partial \mathbf{D}_t}{\partial n}\right) \tag{6}$$

Taking the surface divergence on both sides of (6), and considering the boundary condition of PEC

$$D_n = \rho_s, \tag{7}$$

and the continuity condition of current:

$$\nabla_t \cdot \mathbf{J} = i\omega\rho_s, \tag{8}$$

we have

$$\nabla_t \cdot \mathbf{J} = i\omega\rho_s = \frac{1}{i\omega\mu\varepsilon}\left(\nabla_t^2\rho_s - \nabla_t \cdot \frac{\partial \mathbf{D}_t}{\partial n}\right) \tag{9}$$

Therefore,

$$\nabla_t^2\rho_s + k^2\rho_s = \nabla_t \cdot \frac{\partial \mathbf{D}_t}{\partial n} \tag{10}$$

Equation (10) is an inhomogeneous scalar Helmholtz equation that surface charge should satisfy. Its solution can be expressed as the summation of the general solution of the corresponding homogeneous equation and a particular solution of this inhomogeneous equation.

2.1. The General Solution of the Homogeneous Equation

By solving the homogeneous equation

$$\nabla_t^2 \rho_s + k^2 \rho_s = 0, \tag{11}$$

one can construct the solution with following form:

$$\rho_s = C_m e^{i\mathbf{k}^m \cdot \mathbf{r}}, \tag{12}$$

where $\mathbf{k}^m$ is a vector which amplitude equals to k. Note that in the local rectangular coordinate system ($\hat{\mathbf{u}}$, $\hat{\mathbf{v}}$, $\hat{\mathbf{w}}$), where $\hat{\mathbf{w}} = \hat{\mathbf{u}} \times \hat{\mathbf{v}}$ is the outward unit normal:

$$\mathbf{k}^m = (k_u^m,\, k_v^m,\, k_w^m) \tag{13}$$

$$\mathbf{r} = (u,\, v,\, w) \tag{14}$$

Submitting (12) into (11):

$$-\left[(k_u^m)^2 + (k_v^m)^2\right] C_m e^{i\mathbf{k}^m \cdot \mathbf{r}} + k^2 C_m e^{i\mathbf{k}^m \cdot \mathbf{r}} = 0 \tag{15}$$

Therefore,

$$(k_u^m)^2 + (k_v^m)^2 = k^2 \tag{16}$$

$$k_w^m = 0 \tag{17}$$

Finally, the general solution of this homogeneous equation can be expressed as:

$$\rho_s(\mathbf{r}) = \sum_{m=1}^{M} C_m e^{ik\hat{\mathbf{k}}_t^m \cdot \mathbf{r}}, \tag{18}$$

where $k = \omega\sqrt{\mu\varepsilon}$ is the wave number in free space, and the direction of unit vector $\hat{\mathbf{k}}_t^m$ could be any tangential direction of the PEC surface.

The homogeneous solution does not correspond to the excitation condition. Therefore, it can be considered as the eigen-mode (resonance mode) independent of the excitation.

2.2. The Particular Solution of the Inhomogeneous Equation

According to the boundary condition on PEC surfaces,

$$\mathbf{D}_t(\mathbf{r})|_{\mathbf{r}\in PEC} = \mathbf{D}_t^{inc}(\mathbf{r})\big|_{\mathbf{r}\in PEC} + \mathbf{D}_t^{sca}(\mathbf{r})|_{\mathbf{r}\in PEC} \equiv 0 \tag{19}$$

Note that the tangential component of incident electric flux has the traveling wave phase dependence which can be expressed

as $\mathbf{D}_t^{inc}(\mathbf{r})\big|_{\mathbf{r}\in PEC} \sim e^{ik\hat{\mathbf{k}}^i\cdot\mathbf{r}}$. Due to the phase matching condition implied in (19), the tangential component of scattering electric flux has the same phase dependence $\mathbf{D}_t^{sca}(\mathbf{r})\big|_{\mathbf{r}\in PEC} \sim e^{ik\hat{\mathbf{k}}^i\cdot\mathbf{r}}$ along the PEC surface. So the tangential component of the total $\mathbf{D}$ flux and its partial derivative also have such phase dependence:

$$\mathbf{D}_t(\mathbf{r})\big|_{\mathbf{r}\in PEC} \sim e^{ik\hat{\mathbf{k}}^i\cdot\mathbf{r}} \tag{20}$$

$$\nabla_t \cdot \frac{\partial \mathbf{D}_t}{\partial n} \sim e^{ik\hat{\mathbf{k}}^i\cdot\mathbf{r}} \tag{21}$$

Hence, the right hand side (RHS) of the inhomogeneous Eq. (10) has the phase dependence of traveling wave. It is easy to figure out that ρ_s with the same phase dependence of the RHS *could* be a particular solution of the inhomogeneous equation, which can be expressed as:

$$\rho_s(\mathbf{r}) \sim e^{ik\hat{\mathbf{k}}^i\cdot\mathbf{r}} \tag{22}$$

2.3. The Phase Dependence of the Induced Sources

The general solution of (10) can be written as:

$$\rho_s(\mathbf{r}) = \sum_{m=1}^{M} C_m e^{ik\hat{\mathbf{k}}_t^m\cdot\mathbf{r}} + D(\mathbf{r})\, e^{ik\hat{\mathbf{k}}^i\cdot\mathbf{r}} \tag{23}$$

Due to relationship (8), the induced surface current $\mathbf{J}$ has the same phase dependence.

2.4. Discussions

1 The homogeneous solutions are the eigen solutions, which are decided by the geometry shape of the object, and are independent of excitation condition.

2 This inhomogeneous solution is caused by excitation, including the incident angle and operating frequency.

3 If the shape of object was smooth and convex, the first term of (23) could be neglected and the second term is dominant. However, if there were many edges, corners, or even cavities involved in the object, the first term of (23) turns out to be important and could not be neglected.

Based on the above understanding, for smooth and convex problems, the particular solution of the inhomogeneous equation is

dominant. So we can just consider the propagating wave phase factor in the induced current:

$$\mathbf{J} \sim e^{ik\hat{\mathbf{k}}^i \cdot \mathbf{r}} \tag{24}$$

Therefore, the basis functions with the same traveling wave phase factor as the incident wave are used in this paper to solve scattering from electrically large PEC object involving smooth and convex surface. Termed as Phase Extracted (PE) basis functions, this kind of basis functions can be expressed as the multiplication of an amplitude factor and a phase factor. Considering its accuracy in representing arbitrary curvilinear surfaces, the curvilinear triangular patches are used to discretize the surface of scatterer, and CRWG (curvilinear RWG) functions [25–28] is chosen as the amplitude term of the PE basis functions in this paper because of its excellent performance, while the phase factor is an exponential function as shown in (24). Thus

$$\mathbf{J}(\mathbf{r}) = \mathbf{j}(\mathbf{r}) e^{ik\hat{\mathbf{k}}^i \cdot \mathbf{r}} \tag{25}$$

where $\mathbf{j}(\mathbf{r})$ is the unknown amplitude factor, which can be approximated as the superposition of CRWG basis functions:

$$\mathbf{j}(\mathbf{r}) = \sum_{n=1}^{N} a_n \mathbf{j}_n(\mathbf{r}) \tag{26}$$

where $\mathbf{j}_n(\mathbf{r})$ is CRWG basis functions; $e^{ik\hat{\mathbf{k}}^i \cdot \mathbf{r}}$ is the analytic phase factor.

Multiplying the phase term, the PE basis functions can be finally constructed and the induced current can be expanded with the PE basis functions $\mathbf{j}_n(\mathbf{r}) e^{ik\hat{\mathbf{k}}^i \cdot \mathbf{r}}$:

$$\mathbf{J}(\mathbf{r}) = \sum_{n=1}^{N} a_n \mathbf{j}_n(\mathbf{r}) e^{ik\hat{\mathbf{k}}^i \cdot \mathbf{r}} \tag{27}$$

After the phase extraction, the residual part of the basis needs to express the amplitude distribution only. Compared to the oscillatory phase term, the amplitude term of induced current varies much slower. As a result, they can be defined on much larger mesh patches compared with the traditional basis functions which do not involve any phase information.

3. WIDE BAND CHARACTERISTIC OF PE BASES

Taken account of the phase variation caused by frequency (by means of wave number k), the PE bases have an inborn capacity of describing

the wide band response of a target. For convex objects with smooth surfaces, the phase variation is the main factor that causes the variation of the induced current distribution through different frequencies. Now, such variety has already been expressed by basis functions themselves, leaving amplitude distribution, which is only a slowly varying term, to be described by CRWG functions and their coefficients. As a result, one needs only very small number of unknowns to expand the slowly varying amplitude term of induced current. Namely, one can use only one set of very coarse mesh grid to discretize the objects in the wide frequency range of interest.

In this section, it is shown by two examples that the PE bases can have very accurate computation results obtaining frequency by frequency in a very wide band, which could not be achieved using conventional basis functions without phase information.

Through out the paper, two numerical models are used for examples. They are a PEC sphere with radius of 1.0 m (shown in Fig. 1), and a missile-shaped object with total length of 2.0 m (shown in Fig. 2). The mesh grids are also shown in these two figures, and the mesh densities are 0.125 m and 0.03 m, which are the $\lambda/8$ mesh grids at 300 MHz and 1.25 GHz of the two models, respectively, leading to the numbers of unknowns of 3,528 and 6,387.

MLFMA is employed in order to accelerate the computation and save memory.

In the first example, far field scatterings of model 1 are calculated. The electromagnetic field incidents from the angle $\theta = 0^\circ$, $\varphi = 0^\circ$, and is HH polarized. Responses under three frequency points, 700 MHz, 3700 MHz, and 6700 MHz, are calculated by employing PE bases and Combined Field Integral Equation (CFIE, combination factor is 0.5).

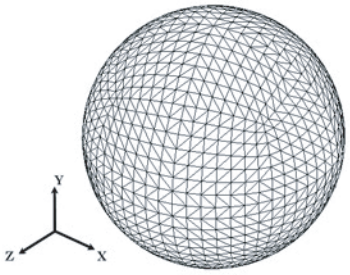

Figure 1. Model 1. PEC sphere with radius of 1.0 m.

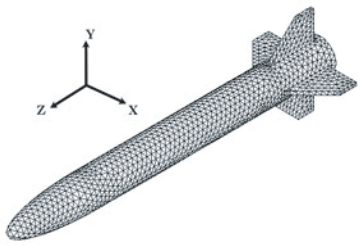

Figure 2. Model 2. PEC missile-shaped object with total length of 2.0 m.

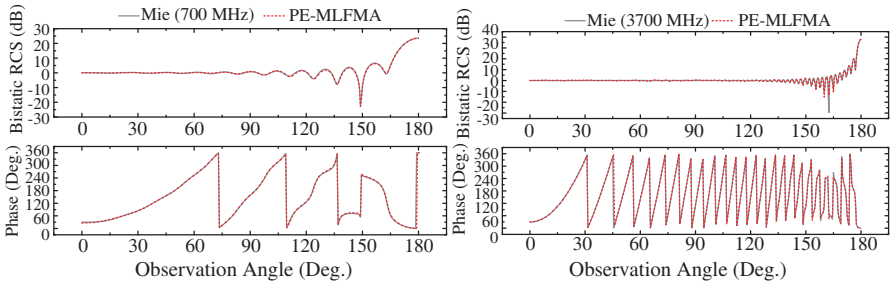

(a) 700 MHz, RMS error of RCS data: 0.2522 dB. (b) 3700 MHz, RMS error of RCS data: 0.9967 dB.

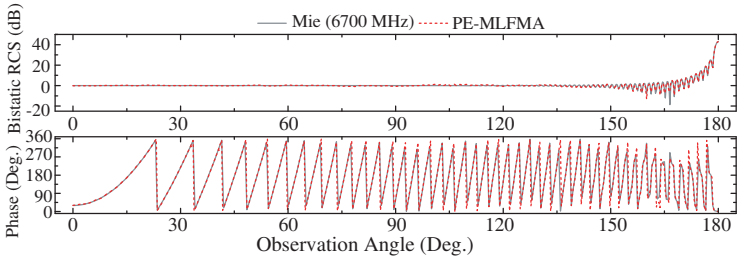

(c) 6700 MHz, RMS error of RCS data: 0.8798 dB.

Figure 3. Far field response of Model 1. PE basis functions use the same coarse mesh grid with unknowns of 3,528.

Using the same mesh density (0.125 m), the electrical radii of the sphere are 2.33λ, 12.33λ, and 22.33λ. And the corresponding electrical patch sizes are about 0.292λ, 1.542λ, and 2.792λ, respectively. Figs. 3(a), (b), and (c) are the far field response at the corresponding frequencies, where the upper one is the result of bistatic RCS and the lower one is the phase distribution of far field, both as a function of observation angle. In these figures, the solid grey lines are results obtained from Mie series, and the dashed red lines are calculated by MLFMA using PE bases. It can be observed that the excellent agreement is obtained in the wide frequency range. The RMS errors of the RCS under these frequencies are only 0.2522 dB, 0.9967 dB, and 0.8798 dB, respectively.

For comparison, the RCS and phase distributions of model 1 under these three frequencies are calculated with traditional CRWG basis functions, using the same mesh grid as PE bases. Figs. 4(a), (b), and (c) show the results. Apparently, CRWG basis functions can obtain correct result only at 700 MHz. However, the RMS error still exceeds 1.0 dB. The results at 3700 MHz and 6700 MHz are totally wrong. In fact, to generate accurate results using CRWG basis functions, one needs to discretize this model to about 400,000, and

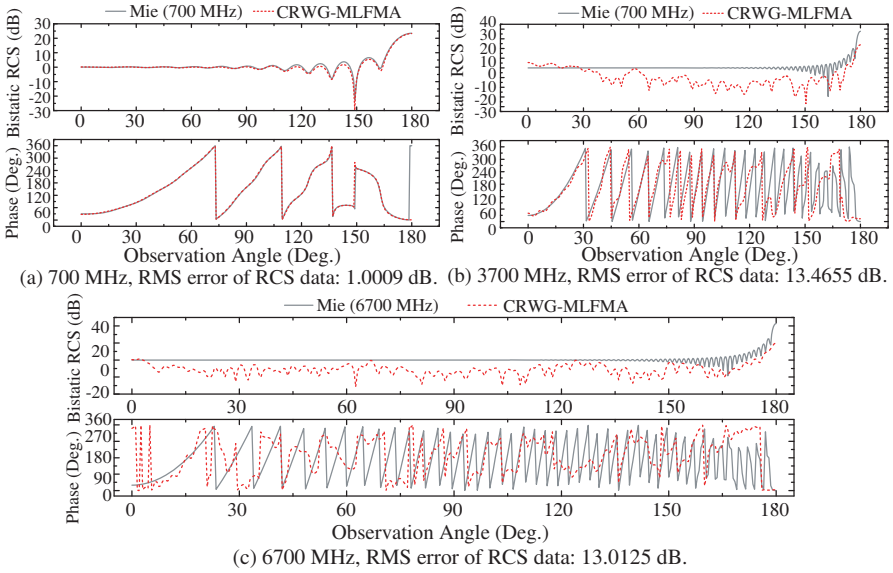

(a) 700 MHz, RMS error of RCS data: 1.0009 dB. (b) 3700 MHz, RMS error of RCS data: 13.4655 dB.

(c) 6700 MHz, RMS error of RCS data: 13.0125 dB.

Figure 4. Far field response of Model 1. CRWG basis functions use the same coarse mesh grid with unknowns of 3,528.

1,400,000 unknowns under the 3700 MHz and 6700 MHz, respectively, far more than 3,528 unknowns needed by PE bases.

Far field responses of model 2 are calculated where the incident fields are set to propagate from the direction $\theta = 90°$, $\varphi = 45°$ (the side of the missile), HH polarized, and the normal direction of scanning plane is set to be $\theta = 90°$, $\varphi = -45°$. Bistatic RCS as well as phase distributions under frequencies 1.50 GHz, 4.50 GHz, and 7.00 GHz are demonstrated in Figs. 5(a), (b), and (c), respectively. Under these three frequencies, the corresponding total electrical lengths of this object are 10.0λ, 30.0λ, and 46.7λ. Employing PE bases and coarse mesh, the electrical patch sizes under the calculation frequencies are 0.15λ, 0.45λ, and 0.70λ, respectively. The results calculated by CFIE (combination factor: 0.5) when using PE bases are shown in dashed red lines, while the referenced results obtained by CRWG bases under fine mesh of 0.10λ under each frequency are illustrated in solid grey lines. In Figs. 5(a) and (b), the solid and dashed lines meet with each other very well, not only the bistatic RCS, but also the phase distributions, showing that very accurate results (real part and imaginary part of far scatter field) can be acquired with PE bases even very coarse mesh is used. Some differences occurred at angle range from 270° to 300° in Fig. 5(c), which makes the overall RMS error slightly big. It is

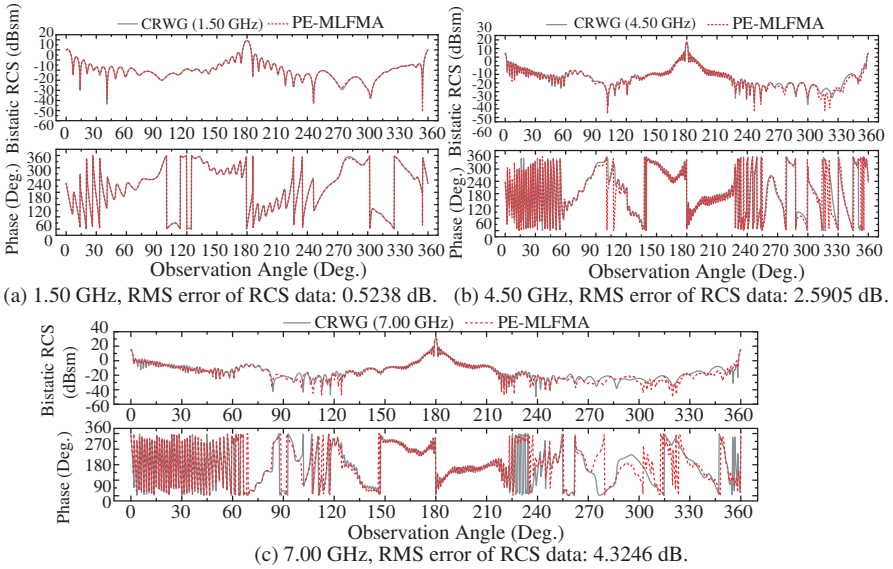

(a) 1.50 GHz, RMS error of RCS data: 0.5238 dB. (b) 4.50 GHz, RMS error of RCS data: 2.5905 dB.

(c) 7.00 GHz, RMS error of RCS data: 4.3246 dB.

Figure 5. Far field response of Model 2. CRWG basis functions use fine mesh grid (0.10λ) under each frequency, while PE basis functions use the same coarse mesh grid with unknowns of 6,387.

because that model 2 is not a rigorous convex smooth target. It has wings and boundaries, which are responsible to these differences and they are small compared with the main lobe of the RCS data. However, in real applications, the very small RCS values are not so important. Generally speaking, the results of model 2 also demonstrate the good accuracy in direct calculation with PE bases under very coarse mesh.

Table 1 lists the computational data of Model 2. Using the same number of unknowns, the PE bases are capable to save several times of memory and CPU time, while do not compromise much accuracy.

From the above examples, it can be concluded that, the PE bases have an excellent characteristic in wide band calculation. A very broad band response could be predicted accurately with the very coarse mesh.

4. INTERPOLATION AND EXTRAPOLATION

As mentioned in Section 1, there are two crucial aspects in a wide band algorithm: (a) the direct calculations at the frequency samples in a wide frequency range, which could be accomplished fast and accurately by solving the integral equations with PE bases, and (b) the reconstructions of concerned quantities at the other frequency points

Table 1. Comparison of computational data for Fig. 5.

Missile-Like (CFIE)	Unknown	Total Iteration Step	Memory Requirement (Mb)	Computational Time (sec.)
PE bases (1.5 GHz)	**6,387**	22	49.1	349
CRWG bases (1.5 GHz)	14,079	25	102.8	1,259
Improvement Ratio	2.20	—	2.09	3.61
PE bases (4.5 GHz)	**6,387**	14	190.6	1,445
CRWG bases (4.5 GHz)	141,930	25	946.6	13,393
Improvement Ratio	22.22	—	4.97	9.27
PE bases (7.0 GHz)	**6,387**	12	394.92	5,208
CRWG bases (7.0 GHz)	323,577	26	2,256.8	29,602
Improvement Ratio	50.66	—	5.71	5.68

using methods such as interpolation or extrapolation, which is to be discussed in this section.

The main idea is that we first solve the scattering problem at some sample frequencies using PE bases and obtain the current coefficients, expressed as a_n in (27), in these frequency samples. This could be achieved by either Method of Moment or any kind of fast algorithm such as MLFMA or Adaptive Integral Method (AIM). Then we use some interpolation and/or extrapolation method to generate current coefficients at other frequency points of interest.

Similar idea can be found in [16] and [17], in which the conventional basis functions are employed to solve the scattering problems at sample frequencies. Since the current coefficients are oscillatory using conventional basis functions, they are "normalized" by a phase factor the same as here involving the PE basis functions. The "normalized" current coefficients are shown to vary very slowly in the frequency range of interest, and could be easily interpolated to other frequency points.

Differently, such phase variation has already been included in the PE basis functions. If PE basis functions, rather than some conventional bases, are used to solve the scattering problems, the resulted current coefficients are already slowly varying quantities, and do not need such "normalization" procedure anymore. As a result, one can directly use a linear or low order polynomial interpolation to generate current coefficients at the frequency points beyond the sample points

In this section, it is first shown that the coefficients of PE bases vary slowly as a function of frequency from the calculation results of model 1 and 2. Then, a simple interpolation and extrapolation method is used to generate current coefficients at other frequencies.

4.1. Current Coefficients at Sample Frequencies

In the following calculations, the mesh grid and excitation settings remain the same as Section 3. Results under sample frequencies are calculated in the brute-force way (directly, frequency by frequency) with PE bases, so that the current coefficient can be examined.

In model 1, responses under 11 frequency samples are calculated. They are from 700 MHz to 6700 MHz with a frequency step of 600 MHz. We randomly choose four basis functions (with basis numbers of 1, 500, 1764, and 2646) to examine their coefficients' variation in the wide frequency band. From Fig. 6, it is clear that the coefficients of these randomly chosen basis functions almost remain unchanged in the broad frequency range from 700 MHz to 6700 MHz, which suggests that it is very easy to have accurate interpolation and extrapolation results at other frequencies. Then the location of the four basis functions has been checked and found that basis number 1764 locates at the lit region of the sphere, and the bases number 1 and 2646 locate at the shadow region, while the 500th basis function happens to locate at the boundary of lit region and shadow region.

Analogy to model 1, we also examine model 2 when the frequency varies from 1.5 GHz to 7.0 GHz, with 12 sample frequencies. Four basis functions (with basis numbers of 1, 1597, 3194, and 4791) are also chosen randomly. The results are shown in Fig. 7. The real parts and imaginary parts all vary very slowly as frequency changes. Then the locations of these basis functions are examined and found that the basis

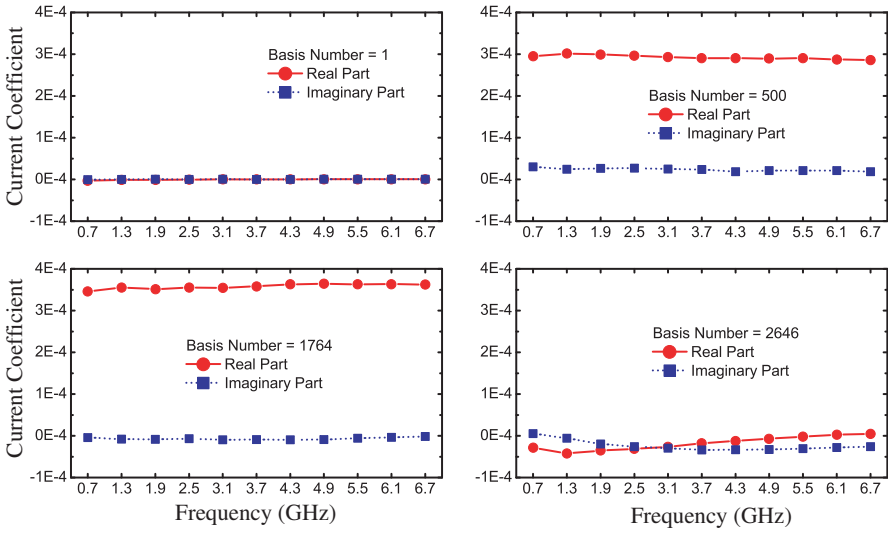

Figure 6. Current coefficient as a function of frequency, Model 1.

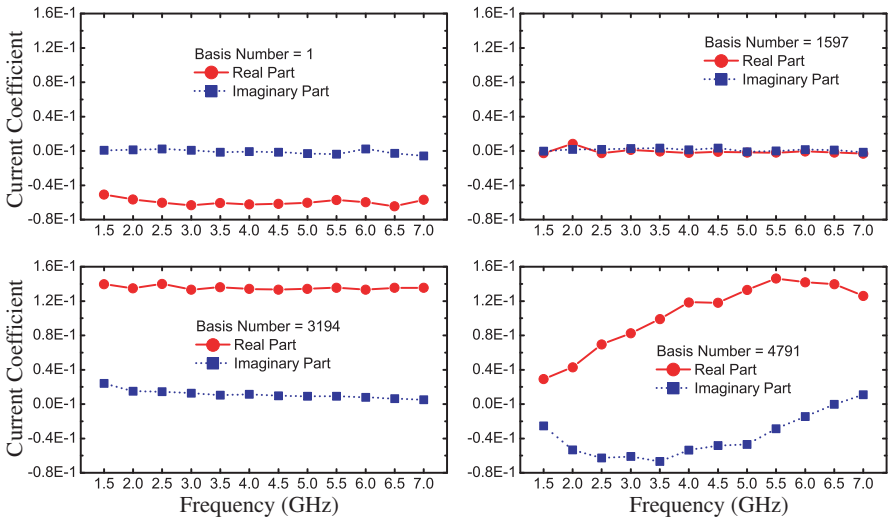

Figure 7. Current coefficient as a function of frequency, Model 2.

functions number 1 and 4791 locate between wings, at shadow region and lit region, respectively, while the 1597th and 3194th basis functions locate at shadow region and lit region, respectively. The variation situations of these bases' coefficients agree with the physics behind their geometry locations well, i.e., when located at the region that has strong multiple coupling, the current coefficient will have stronger variation.

From these discussions, it can be concluded that, after phase extraction, the current coefficients are shown to vary slowly and smoothly. Therefore, either some simple interpolation scheme, such as the linear or low order polynomial interpolation method, or some more complicated ones, Cauchy method for example, could be used here to generate current data on a very broad frequency range based on the current coefficients calculated under sampled frequencies.

4.2. Interpolation and Extrapolation Method

In this paper, a very simple and basic interpolation method, the piecewise cubic Hermite interpolation and extrapolation method [29], is employed in order to preserve the monotonicity and the shape of the data.

Suppose the current coefficients a_n in (27) are continuous functions of frequency $a_n(f)$, $n = 1, 2, \ldots, N$, where N is the number of unknowns. Since the current coefficients are shown to vary smoothly, it

is implied that the first order derivative (with respect to frequency f) of the functions $a_n(f)$ should also be continuous functions. Therefore, we need to construct a cubic polynomial $H_n(f)$ such that:

$$\begin{cases} H_n(f_i) = a_n(f_i) \\ H_n(f_{i+1}) = a_n(f_{i+1}) \\ H'_n(f_i) = a'_n(f_i) \\ H'_n(f_{i+1}) = a'_n(f_{i+1}) \end{cases}, \quad i = 1, 2, \ldots, k-1 \tag{28}$$

In (28), f_i are the sample frequency points, and k is the number of sample frequencies.

In each frequency interval $[f_i, f_{i+1}]$:

$$H_n(f) = a_n(f_i)\alpha_i(f) + a_n(f_{i+1})\,\alpha_{i+1}(f) + a'_n(f_i)\beta_i(f) + a'_n(f_{i+1})\,\beta_{i+1}(f) \tag{29}$$

In (29):

$$\begin{aligned} \alpha_i(f) &= \left(1 + 2\frac{f - f_i}{f_{i+1} - f_i}\right)\left(\frac{f - f_{i+1}}{f_i - f_{i+1}}\right)^2 \\ \alpha_{i+1}(f) &= \left(1 + 2\frac{f - f_{i+1}}{f_i - f_{i+1}}\right)\left(\frac{f - f_i}{f_{i+1} - f_i}\right)^2 \\ \beta_i(f) &= (f - f_i)\left(\frac{f - f_{i+1}}{f_i - f_{i+1}}\right)^2 \\ \beta_{i+1}(f) &= (f - f_{i+1})\left(\frac{f - f_i}{f_{i+1} - f_i}\right)^2 \end{aligned} \tag{30}$$

It is easy to prove that the interpolation polynomial in (29) satisfies the boundary condition (28) within each frequency interval and the connection condition (31) between adjacent intervals:

$$\begin{cases} H_n(f_i - 0) = H_n(f_i + 0) = a_n(f_i) \\ H'_n(f_i - 0) = H'_n(f_i + 0) = a'_n(f_i) \end{cases}, \quad i = 1, \ldots, k \tag{31}$$

In the above expressions (28)–(31), $a_n(f_i)$ are current coefficients at sample frequencies f_i, which can be obtained from solving the scattering problem with PE basis functions. And $a'_n(f_i)$ is the first order derivative of current coefficients at frequency f_i. In practical computation, we simply use frequency difference instead of derivative:

$$a'_n(f_i) \approx \frac{a_n(f_{i+1}) - a_n(f_i)}{f_{i+1} - f_i} \tag{32}$$

Following (29), the current coefficients could be interpolated or extrapolated within or without the overall sample frequency range $[f_{\min}, f_{\max}]$. Considering their slow varying property, the real and imaginary parts of current coefficients are interpolated and extrapolated with such a method independently. And we can consider $H_n(f_j)$ as a good approximation to the actual current coefficients $a_n(f_j)$ at frequency f_j beyond the sample frequencies. Wide band responses can then be calculated using the newly generated coefficients with very high efficiency.

5. WIDE BAND CALCULATION RESULTS

In this section, wide band calculation results of model 1 and 2 are presented in order to demonstrate the good accuracy of the proposed method.

Figure 8(a) shows the forward RCS of model 1. The interpolated results (shown in red circles) from 700 MHz to 6700 MHz are generated based on the sample frequencies (shown in green blocks) the same as those in the previous section. Very good extrapolated results are also obtained from 300 MHz to 700 MHz and from 6700 MHz to 7800 MHz (shown in blue triangles). All results agree very well with the result from Mie series (shown in grey solid line), which is totally covered by data from interpolation and extrapolation. Wide band scattering at another observation angle, 160 degree, has also been illustrated in Fig. 8(b) and all data meet with each other well. From Fig. 8, very accurate results can be obtained using method proposed in this paper at a very wide frequency range with a bandwidth of 1 : 26, while only 11 frequency samples (with a bandwidth of only 1 : 9.57) and only very coarse mesh grid are needed.

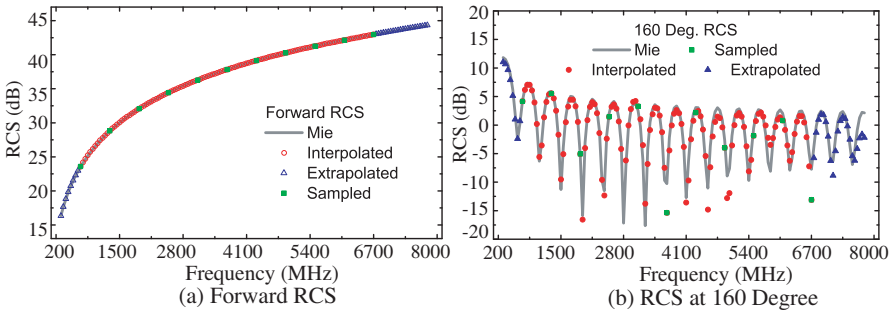

(a) Forward RCS (b) RCS at 160 Degree

Figure 8. Wide band response from 300 MHz to 7800 MHz, Model 1.

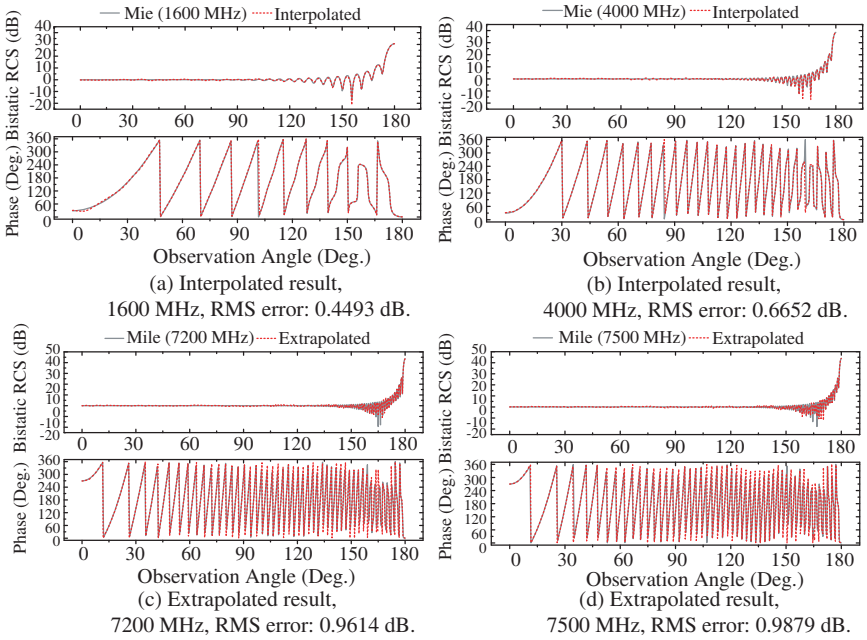

Figure 9. Bistatic RCS and phase distributions at interpolated and extrapolated frequencies, Model 1.

Figures 9(a) and (b) are the interpolated bistatic RCS and phase distribution at 1600 MHz and 4000 MHz, while (c) and (d) represent the extrapolated results at 7200 MHz and 7500 MHz, respectively. All these results are in good agreement with Mie series, with the RMS errors of only 0.4493 dB, 0.6652 dB, 0.9614 dB, and 0.9879 dB, respectively. One more observation from results of model 1 is that after interpolation and extrapolation, the frequency band has been extended of about 25% (from 700 MHz∼6700 MHz to 300 MHz∼7800 MHz).

The wide band responses of model 2 are given in Figs. 10 and 11. Figs. 10(a) and (b) show the forward RCS and RCS at 140 degree, respectively. The interpolated results are from 1.50 GHz to 7.00 GHz with the sample frequencies from 1.5 GHz to 7.0 GHz, with a frequency step of 0.5 GHz (12 frequency samples in total). And the extrapolated results are calculated from 1.00 GHz to 1.45 GHz and from 7.05 GHz to 7.25 GHz. From the Fig. 10(b), we can observe an evident predominance of the interpolation and extrapolation method based on current coefficients. Namely, the method based on current coefficients has the ability to restore the oscillatory property of far field response, which may be lost by methods directly based on far field data.

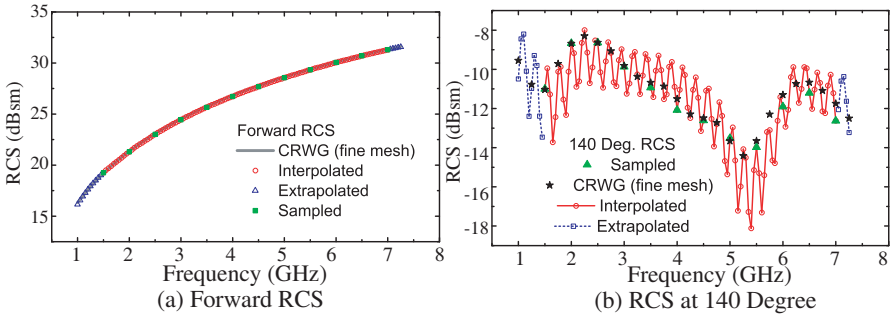

Figure 10. Wide band response from 1.00 GHz to 7.25 GHz, Model 2.

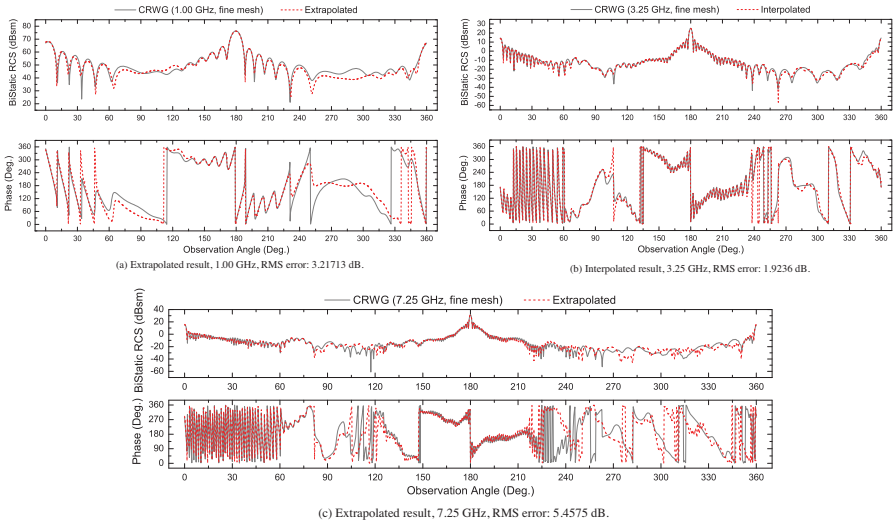

Figure 11. Bistatic RCS and phase distributions at interpolated and extrapolated frequencies, Model 2.

Figures 11(a), (b) and (c) are interpolated and extrapolated bistatic RCS and phase distributions at 1.00 GHz, 3.25 GHz and 7.25 GHz, respectively. All results are compared with accurate solutions obtained from CRWG bases with the 0.125λ mesh data at each frequency. Obviously, they all meet each other well. In this example, the frequency band can be extended from 1 : 4.67 to 1 : 7.25, with a bandwidth extension of about 13.6%.

6. DISCUSSIONS

From the investigations in the previous sections, it can be concluded that the proposed wide band method can reduce the computational time and memory requirement dramatically:

(1) Due to the use of PE basis functions and MLFMA, the computational time and memory requirement in the brute-force calculation at sample frequency points can be reduced by several times compared with method using traditional basis functions, as shown in Table 1.

(2) The interpolation and extrapolation are simple to implement, and very little time is needed in this procedure which could be neglected.

(3) The reconstruction procedure does not need to solve the integral equation, since the current coefficients have already obtained. Therefore, reconstruction procedure is also effective and does not need much CPU time and memory.

Some comparisons can be made to show the advantages of proposed method in this paper:

(1) Compared with methods involving the entire impedance matrix, such as AWE/Padé approximation [1, 2], MBPE method [6–8], and impedance interpolation method [9, 10], the proposed method avoids the handling of full impedance matrix. Apparently, in a real world application, which may involve millions of unknowns (for instance, the case shown in Fig. 3(c) and Fig. 4(c)), it is impossible to generate and store the entire impedance matrix. Differently, the proposed method only needs to solve the scattering problem at some sample frequency points, which could be achieved by any method like MoM, MLFMA, Conjugate Gradient - Fast Fourier Transform (CG-FFT), or AIM.

(2) Compared with Cauchy method [3–5], which can also be based on the interpolation of current coefficients, the proposed interpolation method is much more simple to implement. The interpolation polynomial has explicit formula which could be handled with ease. However, the Cauchy method generally needs to solve a total least square (TLS) problem with Singular Value Decomposition (SVD), which could be rather complicated. This advantage of proposed method is achieved by the use of the PE basis functions, which leads to a rather slowly and smoothly varying data. In fact, many other interpolation methods such as piecewise linear interpolation, cubic spline interpolation method [30] can also be used besides the piecewise cubic Hermite interpolation method used in this paper.

(3) Compared with method introduced in [16] and [17], the method proposed in this paper needs much less unknowns in direct calculation. The mesh grid could be generated only once at the lowest frequency of interest. This leads to much less work in geometrical modeling which would be rather complicated in real world applications. Moreover, the proposed method in this paper does not need the "normalization" process, thanks to the PE basis functions.

At the same time, owing to the limitation of PE basis functions, the proposed method also has some inconvenience when the object has some strong multiple coupling structures such as edges or cavities, because the homogenous solution (18) cannot be neglected in such case. Apparently, it is not enough to express the actual phase variation with only PE basis functions. To overcome this problem, some homogeneous solutions should also be taken into account to construct a more complete basis set. This would be the next work of our research.

7. CONCLUSION

In this paper, the wide band characteristic of PE bases has been investigated and applied to analyze the wide band scattering from PEC objects. By employing PE basis functions, the scattering problem can be solved with much less memory consuming and CPU time in the brute-force way. And the resulted current coefficients vary very slowly with frequency changing, which allows us to use a very simple interpolation and extrapolation method to obtain the current coefficients at other frequency points beyond the sample points. With the proposed method, very high precision can be observed in the calculation of both amplitude and phase distributions of the scattering far field in the numerical examples. As a result, wide band radar response from electrically large PEC targets can be calculated efficiently and accurately with the method reported in this paper.

ACKNOWLEDGMENT

This work was supported partially by National Natural Science Foundation of China under Contract No. 60431010, and 973 Program under Contract No. 6136001, partially by the 111 project under Contract No. B07046.

REFERENCES

1. Reddy, C. J., M. D. Deshpande, C. R. Cockrell, and F. B. Beck, "Fast RCS computation over a frequency band using method of moments in conjunction with asymptotic waveform evaluation technique," *IEEE Trans. Antennas Propagat.*, Vol. 46, No. 8, 1229–1233, Aug. 1998.
2. Erdemli, Y. E., J. Gong, C. J. Reddy, and J. L. Volakis, "Fast RCS pattern fill using AWE technique," *IEEE Trans. Antennas Propagat.*, Vol. 46, No. 11, 1752–1753, Nov. 1998.
3. Adve, R. S., T. K. Sarkar, S. M. Rao, E. K. Miller, and D. R. Pflug, "Application of the cauchy method for extrapolating/interpolating narrow-band system responses," *IEEE Trans. Microw. Theory Tech.*, Vol. 45, No. 5, 837–845, May 1997.
4. Yang, J. and T. K. Sarkar, "Interpolation/extrapolation of radar cross-section (RCS) data in the frequency domain using the cauchy method," *IEEE Trans. Antennas Propagat.*, Vol. 55, No. 10, 2844–2851, Oct. 2007.
5. Tong, C., N. Yuan, Y. Cao, and W. Hong, "A fast frequency sweeping method for RCS computation based on the rational interpolation technique," *2002 3rd International Conference on Microwave and Millimeter Wave Technology Proceedings*, 2002.
6. Miller, E. K., "Model-based parameter estimation in electromagnetics: Part I. Background and theoretical development," *IEEE Antennas Propag. Mag.*, Vol. 40, No. 1, Feb. 1998.
7. Miller, E. K., "Model-based parameter estimation in electromagnetics: Part II. Applications to EM observables," *IEEE Antennas Propag. Mag.*, Vol. 40, No. 2, Apr. 1998.
8. Miller, E. K., "Model-based parameter estimation in electromagnetics: Part III. Applications to EM integral equations," *IEEE Antennas Propag. Mag.*, Vol. 40, No. 3, Jun. 1998.
9. Newman, E. H., "Generation of wide-band data from the method of moments by interpolating the impedance matrix," *IEEE Trans. Antennas Propagat.*, Vol. 36, No. 12, 1820–1824, Dec. 1988,.
10. Yeo, J. and R. Mittra, "Fast computation of MOM matrix elements over a wide frequency range using a new interpolation technique," *IEEE MTT-S*, Vol. 3, 1979–1982, 2003.
11. Prakash, V. V. S., "RCS computation over a frequency band using the characteristic basis and model order reduction method," *IEEE Antennas and Propagation Society International Symposium*, Vol. 4, 89–92, 2003.
12. Rui, P. L., R. S. Chen, Z. W. Liu, and Y. N. Gan, "Schwarz-Krylov

subspace method for MLFMM analysis of electromagnetic wave scattering problems," *Progress In Electromagnetics Research*, PIER 82, 51–63, 2008.

13. Zhang, Y. J. and E. P. Li, "Fast multipole accelerated scattering matrix method for multiple scattering of a large number of cylinders," *Progress In Electromagnetics Research*, PIER 72, 105–126, 2007.
14. Wan, J. X., T. M. Xiang, and C. H. Liang, "The fast multipole algorithm for analysis of large-scale microstrip antenna arrays," *Progress In Electromagnetics Research*, PIER 49, 239–255, 2004.
15. Pan, Y. C. and W. C. Chew, "A fast multipole method for embedded structure in a stratified medium," *Progress In Electromagnetics Research*, PIER 44, 1–38, 2004.
16. Lu, C. C., "A simple extrapolation method based on current for rapid frequency and angle sweep in far-field calculation of an integral equation algorithm," *IEEE/ACES International Conference on Wireless Communications and Applied Computational Electromagnetics*, 333–336, 2005.
17. Lu, C. C., "An extrapolation method based on current for rapid frequency and angle sweeps in far-field calculation in an integral equation algorithm," *Applied Computational Electromagnetics Society Journal*, Vol. 21, No. 1, 90–98, Mar. 2006.
18. Hatamzadeh-Varmazyar, S., M. Naser-Moghadasi, and Z. Masouri, "A moment method simulation of electromagnetic scatter ing from conducting bodies," *Progress In Electromagnetics Research*, PIER 81, 99–119, 2008.
19. Wang, S., X. Guan, D. Wang, X. Ma, and Y. Su, "Electromagnetic scattering by mixed conducting/dielectric objects using higher order MOM," *Progress In Electromagnetics Research*, PIER 66, 51–63, 2006.
20. Li, C. and Z. Shen, "Electromagnetic scattering by a conducting cylinder coated with metamaterials," *Progress In Electromagnetics Research*, PIER 42, 91–105, 2003.
21. Yuan, H. W., S. X. Gong, X. Wang, and W. T. Wang, "Scattering analysis of a printed dipole antenna using PBG structures," *Progress In Electromagnetics Research B*, Vol. 1, 189–195, 2008.
22. Varmazyar, S. H. and M. N. Moghadasi, "An integral equation modeling of electromagnetic scattering from the surfaces of arbitrary resistance distribution," *Progress In Electromagnetics Research B*, Vol. 3, 157–172, 2008.
23. Varmazyar, S. H. and M. N. Moghadasi, "New numerical method

for determining the scattered electromagnetic fields from thin wires," *Progress In Electromagnetics Research B*, Vol. 3, 207–218, 2008.

24. Nie, Z., S. Yan, S. He, and J. Hu, "On the basis functions with traveling wave phase factor for efficient analysis of scattering from electrically large targets," *Progress In Electromagnetics Research*, PIER 85, 83–114, 2008.
25. Graglia, R. D., D. R. Wilton, and A. F. Peterson, "Higher order interpolatory vector bases for computational electromagnetics," *IEEE Trans. Antennas Propagat.*, Vol. 45, No. 3, 329–342, Mar. 1997.
26. Wilkes, D. L. and C.-C. Cha, "Method of moments solution with parametric curved triangular patches," *Antennas and Propagation Society International Symposium*, Vol. 3, 1512–1515, Jun. 1991.
27. Zhu, N. Y. and F. M. Landstorfer, "Application of curved parametric triangular and quadrilateral edge elements in the moment solution of the EFIE," *IEEE Microwave and Guided Wave Letters*, Vol. 3, No. 9, 319–321, Sep. 1993.
28. Brown, W. J. and D. R. Wilton, "Singular basis functions and curvilinear triangles in the solution of the electric field integral equation," *IEEE Trans. Antennas Propagat.*, Vol. 47, No. 2, 347–353, Feb. 1999.
29. Fritsch, F. N. and R. E. Carlson, "Monotone piecewise cubic interpolation," *SIAM Journal on Numerical Analysis*, Vol. 17, 238–246, 1980.
30. De Boor, C., *A Practical Guide to Splines*, Springer-Verlag, 1978.